Appl. Phys. B 62, 153–158 (1996)

Applied Physics B Lasers and Optics



# Power and beam-width dependence of a $BaTiO_3$:Ce self-pumped phase conjugator

**H. Gao, S.X. Dou, J. Zhang, Y. Zhu, P. Ye**

Institute of Physics, Chinese Academy of Sciences, P.O. Box 603, Beijing 100080, People's Republic of China
(Fax: + 86-10/2562605)

Received: 19 January 1995/Accepted: 3 May 1995

**Abstract.** Power and beam-width dependences of the performance of self-pumped phase conjugators using a $BaTiO_3$:Ce crystal have been investigated. The incident beam was permitted to enter the crystal by the *a*-face or the + *c*-face. In both cases, the phase-conjugate reflectivity was observed to vary with the power and beam width of the incident beam. In the former case, two different optical beam patterns in the crystal can be observed under different conditions. Qualitative explanations are given to some of the results observed.

**PACS:** 42.65.Hw

Self-pumped phase conjugators using photorefractive crystals [1, 2] have been intensively studied since their first demonstrations in 1982 [3, 4]. Photorefractive crystals can produce phase-conjugate replica of a laser beam at low cw power. This feature makes it possible for photorefractive phase conjugators to find applications in many fields where the wavefront-reversing properties are required [5].

Although Self-Pumped Phase Conjugation (SPPC) can be generated in photorefractive crystals with both external [3] and internal [4] geometries, internal geometry is usually preferred for its ease of use, compactness and relaxation of optical alignment requirement. In internal self-pumped phase conjugators, it has been generally believed that there are mainly two typical mechanisms responsible for the establishment of SPPC. One is Total Internal Reflection (TIR) [4], the other is Stimulated Photorefractive Backscattering (SPB) [6]. With the former, SPPC is established through self-generated Four-Wave Mixing (FWM) interactions, for which the two pump beams are the fanning beam (amplified forward scattering light) and the returned fanning beam through successive reflections on the neighbouring faces near a crystal corner. With the latter, the SPPC is established by only relying on SPB interaction: the phase-conjugate signal is the amplified backscattered noisy light in the presence of the incident beam. It should be noted that the process of SPPC generation with SPB mechanism was observed only in few experiments [6, 7].

With the gradual appearance of different doped crystals during the past several years, it was found that a new typical mechanism, Stimulated Photorefractive Backscattering and Four-Wave Mixing (SPB-FWM), often dominates in the doped phase conjugators when the usual TIR beam-crystal geometry is used [8–11]. With this new mechanism, the SPPC is also established through FWM interactions, but for which one pump beam (the returned fanning beam) is produced by SPB amplification of backscattered light in the presence of the fanning beam, rather than by TIR. The reason for the frequent dominance of the SPB-FWM mechanism in doped phase conjugators is that doped crystals have enhanced SPB gain coefficients (or contra-directional two-beam coupling gain coefficient), $\gamma_{2k}$, compared to undoped crystals [12]. The most notable characteristic of a SPB-FWM phase conjugator is that, unlike in a TIR one, the fanning beam does not have to be directed toward a crystal corner for the establishment of SPPC.

It is well known that at a fixed beam-crystal geometry, the efficiency of a self-pumped phase conjugator depends on the optical parameters of the incident beam, such as wavelength, beam width and power (or intensity). These parameters are important because their variations may cause the changes of photorefractivity and absorption of the crystal, of interaction lengths of the FWM regions.

In this paper, we present our investigations of the performances (efficiency, response time) of a SPB-FWM $BaTiO_3$:Ce phase conjugator (the beam being incident on an *a*-face of the 0°-cut crystal) and, for comparison, of TIR phase conjugator (the beam being incident on the + *c*-face of the crystal) as functions of power and beam width of the incident beam. In comparison with undoped crystal, $BaTiO_3$:Ce has improved SPPC properties in the whole visible wavelength range

and at short wavelengths in the near-infrared [10, 11]. Two-beam coupling experiments have demonstrated the close correlation between the Ce concentration and the gain coefficient [13].

We have observed that, depending on the parameters of the incident beam, two distinct beam patterns that generate SPPC can be formed in the SPB-FWM phase conjugator. This phenomenon was neither observed in the present TIR phase conjugator nor in other previously studied TIR phase conjugators using undoped $BaTiO_3$ crystals. In TIR phase conjugators, one of the beam patterns mentioned above cannot generate SPPC: the FWM interactions diminish as long as the fanning beam deviates from the relevant crystal corner [14, 15]. Our experiments clearly demonstrate the importance of the power and, especially, the beam width in determining the beam path patterns, efficiency and time response of our SPB-FWM phase conjugator.

## 1 Experiments and results

The $BaTiO_3$ : Ce crystal that we used in the experiments has a Ce-doping concentration of 8 parts in $10^6$ and is red-orange. It was poled and 0°-cut with dimensions of 6.8 mm × 6.2 mm × 6.3 mm. Its 6.8 mm long edge was along the $c$-axis. All six faces of the crystal have been well polished.

The light source in the SPPC experiments was a rhodamin DCM dye laser pumped with an $Ar^+$ laser. After it passed through an optical isolator, the horizontally polarized laser was focused onto the crystal by the use of a lens of 60 cm focal length. The diameter of the focused beam on the crystal was varied by displacing the lens. To measure the power of the incident beam and the phase-conjugate signal, a beam splitter was inserted in the laser beam path between the lens and the crystal. The optical beam path patterns in the crystal was observed on a monitor by the used of a CCD camera. The wavelength used is 665 nm at which the absorption coefficient of the crystal is about 0.2 $cm^{-1}$.

### *1.1 Geometry with the beam entering the crystal by an a-face*

In this part of our experiments, the crystal was so positioned that the laser beam entered the crystal by one of its $a$-faces with $e$-polarization. Its propagation direction in the crystal lay in the $a-c$ principal plane and made an acute angle with the direction of the $c$-axis. The external incident angle $\theta$ was fixed at 55°. The distance between the incident position and the bottom face of the crystal was 4.5 mm.

In our experiments, it was observed that the optical beam patterns in the phase conjugator varied with the incident Gaussian beam radius $\omega_0$ when the incident power $P$ was fixed. With thin beams, the fanning beams often converged on one bottom crystal corner. A typical result is given in Fig. 1a. In this case, the establishment of SPPC relies on SPB-FWM mechanism with the bottom crystal corner providing the backscattering seeding beam for the SPB interaction that exists between the fanning beam and the backward-propagating beam.

With thick beams, on the other hand, the fanning beam no longer touches the bottom crystal corner. Rather, it propagates towards the bottom crystal face and touches one top crystal corner after two successive reflections. A typical photograph of this kind of beam patterns is presented in Fig. 1b. In this case, the SPPC mechanism is also SPB-FWM. The SPB interaction between the fanning beam and backward-propagating beam, however, relies on the seeding provided by the top crystal corner with total internal reflections.

With beams of medium sizes, the beam patterns often varied between the corner patterns and the face patterns. The phase-conjugate signal cannot arrive at the steady state; rather, it is self-pulsing.

All the above phenomena can be qualitatively explained by considering that the FWM coupling strength $\gamma l$ in the crystal varied with the beam radius of the incident Gaussian beam $\omega_0$. This will be discussed in Sect. 2.

The SPPC reflectivity $R$ of the phase conjugator has been measured during the above experiments. The results are shown in Fig. 2. At each incident power, $R$ increases

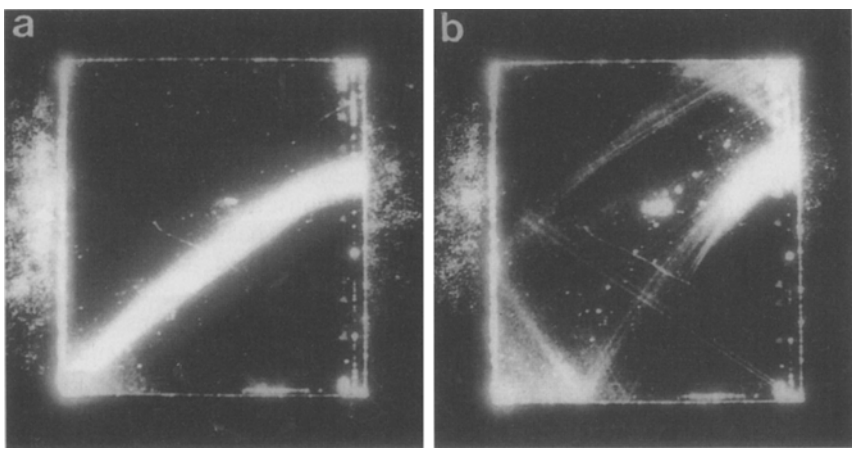


**Fig. 1a, b.** Photographs of the two beam patterns that were observed in the $a$-face-incidence phase conjugator. **a** Corner patters; **b** face patterns. The direction of the $c$-axis of the crystal is from *top* to *bottom*. The pump beam enters the crystal by the right face at $X = 4.5$ mm, $\theta = 55°$, where $X$ is the distance from bottom to the incident position–$\theta$ is the external incident angle

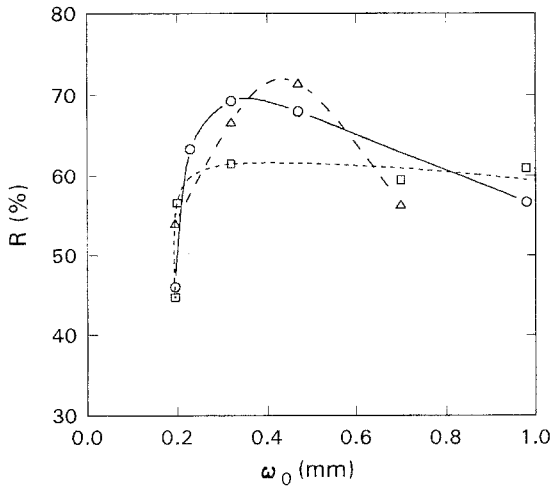


**Fig. 2.** SPPC reflectivity $R$ vs beam width $\omega_0$ at different incident powers of the $a$-face-incidence phase conjugator, △, P = 30 mW; ○, $P$ = 35 mW; □, $P$ = 50 mW. The *lines* are guides to the eye

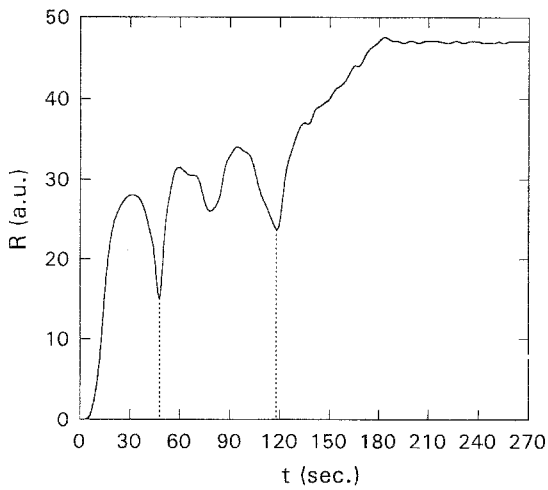


**Fig. 3.** Typical time evolution of SPPC reflectivity of $a$-face-incidence phase conjugator when SPPC was first established with corner patterns ($t < \sim 48$ s) and then with face patterns ($t > \sim 116$ s). Between 48 and 116 s, the beam patterns were unstable and varying between corner patterns and face patterns. $\omega_0 = 0.32$ mm, $P = 35$ mW

and then decreases with $\omega_0$. An optimum $\omega_0$ exists for each power.

With fixed $\omega_0$, we have investigated the efficiency of SPPC generation in the phase conjugator at different powers. With thin beams ($\omega_0 < 0.3$ mm) it was observed that the SPPC generation relies on the bottom crystal corner in most cases. With thick beams ($\omega_0 > 0.4$ mm), the contrary is true: the SPPC generation almost always corresponds to the face-patterns, regardless of the incident power.

When $\omega_0$ is between 0.3 and 0.4 mm, it was observed that the SPPC generation corresponds to corner patterns or face patterns, depending on $P$. When $P$ is very low or very high, corner patterns appeared in the phase conjugator. When $P$ is between about 20 and 35 mW, however, face patterns dominated in the phase conjugator. It should be noted that in these cases corner patters usually appeared at earlier times: after a certain time interval in which the beam patterns were unstable and varying between corner and face patterns due to competition, face patterns become dominant. Accordingly, $R$ has a corresponding increase from a lower level to a higher level. A typical time evolution of the phase-conjugate signal is presented in Fig. 3. This variation of beam patterns means that SPPC is more easily established with corner patterns. But face patterns will appear at last due to the fact that they generate SPPC more efficiently than the corner pattern.

The variations of $R$ with $P$ at fixed $\omega_0$ are given in Fig. 4. It can be noticed that at each $\omega_0$, $R$ increases with $P$ and then tends to be saturated. With small $\omega_0$, $R$ decreases with $P$ when $P$ is high. The thinner the beam is, the earlier $R$ saturates.

The response time of the phase conjugator has been measured at different $\omega_0$ and $P$. The results are given in Fig. 5. At fixed $\omega_0$, the rise time is linearly proportional to $1/P$. At fixed $P$, it decreases with $\omega_0$. This should result from the fact that fanning effect that is important in the establishment of SPPC is more strong with thick beams.

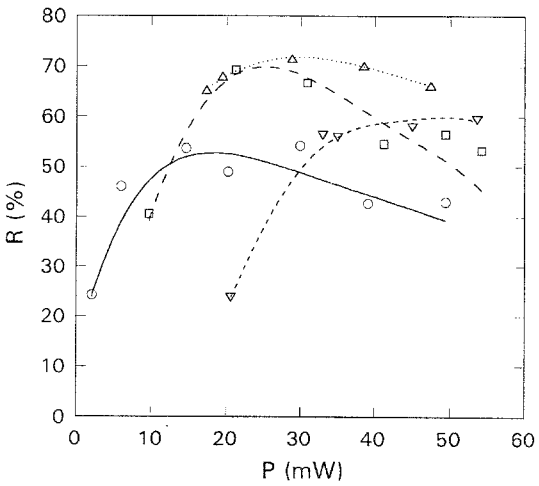


**Fig. 4.** $R$ vs $P$ of the $a$-face-incidence phase conjugator at different beam widths, ○, $\omega_0 = 0.20$ mm; □, $\omega_0 = 0.32$ mm; △, $\omega_0 = 0.47$ mm; ▽, $\omega_0 = 0.70$ mm

### *1.2 Geometry with the beam entering the crystal by its + c-face*

In this part of our experiments, the incident beam was permitted to enter the crystal by the + $c$-face. This corresponds to the fact that the $c$-axis is from left to right in Fig. 1. The incident angle was 22°, and the distance between the incident position and bottom face was 4.0 mm. It this case, the beam patterns are similar to the corner patterns as shown in Fig. 1. It should be noted that the SPPC mechanism is TIR in this case. The SPB interaction between the fanning beam and the beam propagating back to the FWM region increases the energy loss of these beams and is detrimental to the SPPC generation. This is contrary to the $a$-face-incident case. Thus, it should be

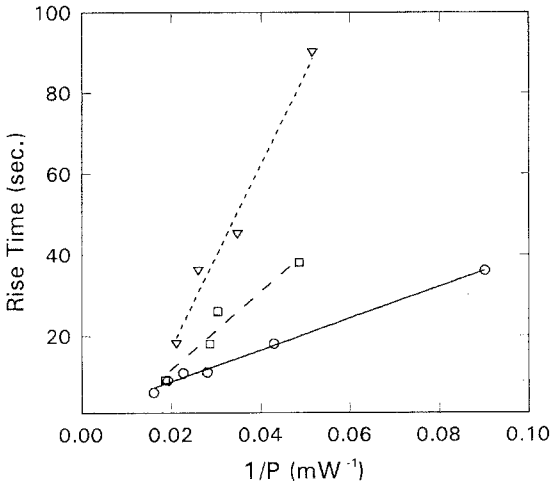


**Fig. 5.** The rise time vs $1/P$ of the $a$-face-incidence phase conjugator at different beam widths. ▽, $\omega_0 = 0.47$ mm; □, $\omega_0 = 0.70$ mm; ○, $\omega_0 = 0.98$ mm

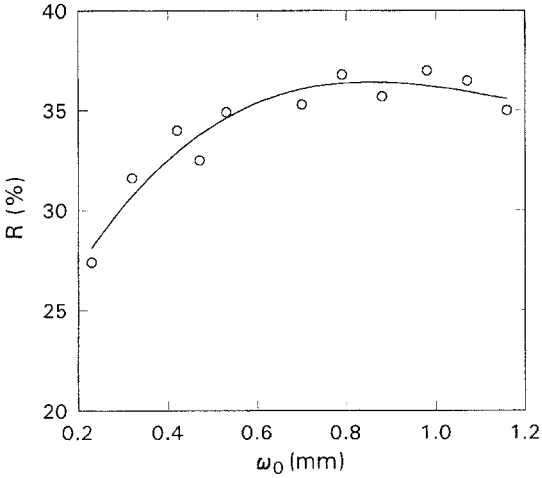


**Fig. 6.** $R$ vs $\omega_0$ of the $+c$-face-incidence phase conjugator; $P = 30$ mW

expected that the power and beam radius dependence of the SPPC generation should be different between the two cases.

In Fig. 6, the $\omega_0$-dependence of $R$ at fixed $P$ is shown. It can be seen from Fig. 6 that $R$ increases with $\omega_0$ in a large range. Then it saturates. The difference between Figs. 2 and 6 is obvious. This could be explained by considering the differences in the SPPC mechanisms (see Sect. 2).

The $P$-dependence of $R$ at fixed $\omega_0$ is measured. It was found that $R$ increases with $P$ and then saturates. A typical result is shown in Fig. 7.

In our experiments, we have noticed that the time evolution of the phase-conjugate signals in the two types of phase conjugators are somewhat different in the same experimental conditions ($P$ and $\omega_0$). One typical result is shown in Fig. 8. With both phase conjugators, the signal power increases and saturates with $t$. But for the $+c$-face-incidence phase conjugator, the increase of the signal power slows down after it reaches about half of its maximum. We believe this is due to the fact that the establishment of SPPC only relies on FWM and total internal reflection at the early stage. With time going on, the SPB interaction that is detrimental to the SPPC process gradually becomes stronger. In the $a$-face-incidence phase conjugator, on the other hand, the strengthening SPB interaction only accelerates the saturation of the signal power.

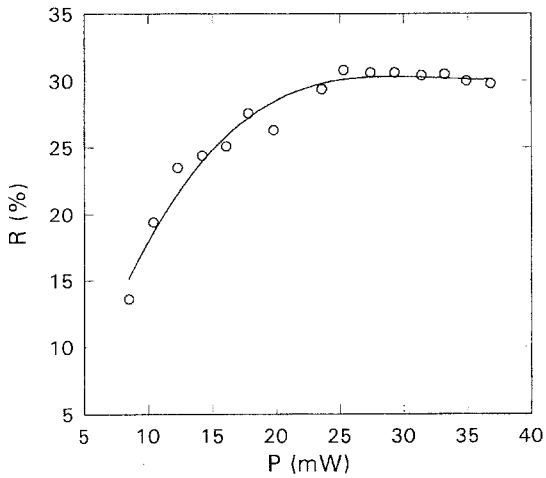


**Fig. 7.** $R$ vs $P$ of the $+c$-face-incidence phase conjugator; $\omega_0 = 0.23$ mm

## 2 Discussion

The interacting waves in the phase conjugators that correspond to Fig. 1 are schematically shown in Fig. 9. As the SPB interaction region provides feedback for the FWM interaction by amplifying and backscattering wave at the expense of the fanning wave, a SPB-FWM phase conjugator is similar to a semi-linear passive phase conjugator. Neglecting the SPB interaction between beams 1 and 2 in the FWM region, the efficiency $R$ of such a phase

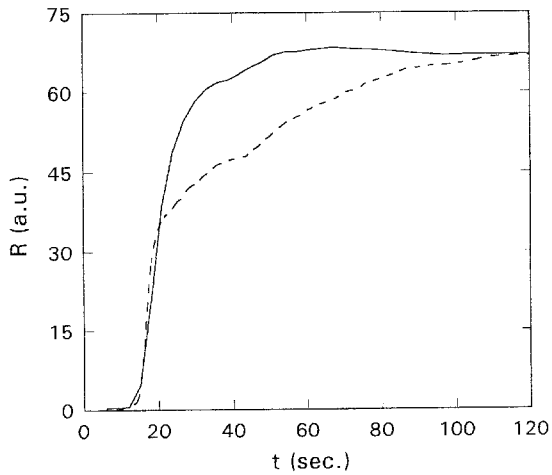


**Fig. 8.** Time evolution of SPPC reflectivity. $P = 30$ mW, $\omega_0 = 0.47$ mm. —, $a$-face-incidence; - - - -, $+c$-face-incidence

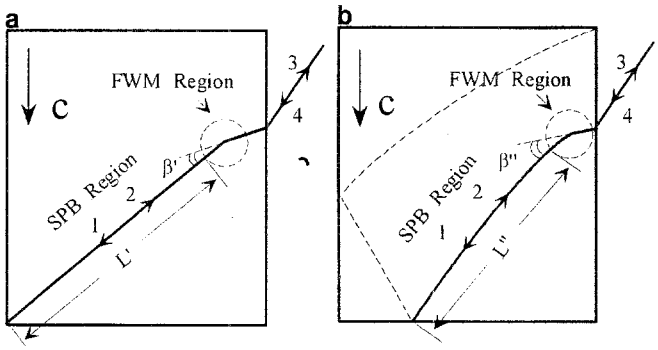


**Fig. 9a,b.** Interacting waves in the phase conjugators that correspond to Fig. 1 *Beam 1* and *2* are, respectively, the fanning beam and the backward-propagating beam. *Beam 3* is the phase-conjugate signal for the incident *beam 4*. $\beta(\beta' \text{or} \beta'')$ is the angle between *beams 1* and *4*. $L(L' \text{or} L'')$ is the SPB interaction length

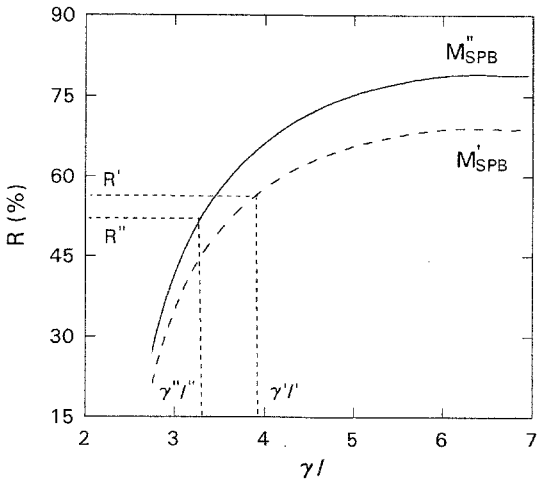


**Fig. 10.** $R$ of a SPB-FWM phase conjugator as a function of the FWM coupling strength $\gamma l$ at two values of $M_{SPB}$ ($M''_{SPB} > M'_{SPB}$)

conjugator is determined by the FWM coupling strength $\gamma l$ and the reflectivity $M_{SPB}$ generated by the SPB region in the following way [16]:

$$R = \left( \frac{M_{SPB}^{1/2} + [a^2(1 + M_{SPB}) - 1]^{1/2}}{M_{SPB} + 2 - M_{SPB}^{1/2}[a^2(1 + M_{SPB}) - 1]^{1/2}} \right)^2, \quad (1)$$

with $a$ satisfying

$$\tanh\left(\frac{\gamma l}{2} a\right) = a. \quad (2)$$

Among the three parameters $\gamma$, $l$ and $M_{SPB}$, $\gamma$ is a function of the angle $\beta$ [17] and of the light intensity $I$ [13, 18] ($\gamma$ usually increases and then saturates with $I$). The effective FWM interaction length $l$ depends on the overlapping area of the interacting beams and thus is a function of $\omega_0$ and $\beta$ [19]: $l$ should increase with $\omega_0$ and decrease with $\beta$.

$M_{SPB}$ is a function of $\gamma_{2k}$, $L$, $\alpha$ (absorption coefficient) and the seeding reflection $R_S$ of the crystal corner. By using the approximate solution for SPB interaction given in [20], one can obtain

$$M_{SPB} = [(\sqrt{S} - 1)/(\sqrt{S} + 1)] \exp(-\alpha L), \quad (3)$$

with $S$ being defined as

$$S = 1 + 4R_S \exp(-\alpha L)[1 - R_S \exp(-\alpha L)]^{-2} \times \exp(2\gamma_{2K} L). \quad (4)$$

To see the effect of absorption in the SPB region, we compare two extreme cases: $\gamma_{2K} \approx 0$ and $\gamma_{2K} \gg 0$. It can be seen that if $\gamma_{2K} \approx 0$, one has $M_{SPB} \propto \exp(-2\gamma_{2K} L)$. Thus, the effect of absorption can be partially diminished due to the SPB interaction, and the higher $\gamma_{2K} L$ is, the less is the effect of absorption.

Knowing the roles of power, beam width, etc., in the variation of $\gamma$, $l$ and $M_{SPB}$, we find that some of the experimental phenomena observed in our experiments can be qualitatively explained.

In the case of $a$-face-incidence configuration, if we designate the parameters of the phase conjugator with corner patterns (face patters) as $\gamma'(\gamma'')$, $l'(l'')$, etc. Then it can be known from calculation that $\gamma' > \gamma''$, $\gamma'_{2k} < \gamma''_{2k}$. For example, with a charge carrier density of $2 \times 10^{17}$ cm$^{-3}$, $\gamma'(\gamma'')$ is estimated to be 3.3 mm$^{-1}$ (3.0 mm$^{-1}$), and $\gamma'_{2k}(\gamma''_{2k})$ is 1.3 mm$^{-1}$ (1.6 mm$^{-1}$). As $l'$ is large than $l''$, we can surely know hat $\gamma' l' > \gamma'' l''$. As to $\gamma'_{2k} L'$ and $\gamma''_{2k} L''$, we also have $\gamma'_{2k} L' < \gamma''_{2k} L''$ due to the fact that $L'(= 6.1$ mm) is only slightly larger than $L''$ ($= 5.4$ mm, which corresponds to the distance between the FWM region and the point where the fanning beam touches the bottom crystal face; the backward-propagating beam experiences SPB gain only in this region). From the fact that the fanning beam is depleted in a short distance in the case of face patterns, whereas it is not in the case of corner patterns (Fig. 1), it is evident that the actual difference between $\gamma'_{2k} L'$ and $\gamma''_{2k} L''$ is larger than predicted and that the energy loss of beams 1 and 2 from absorption is more serious in the case of corner patterns. Thus, we have $M'_{SPB} < M''_{SPB}$.

At a fixed $M_{SPB}$, $R$ of a SPB-FWM phase conjugator at different $\gamma l$ can be calculated theoretically by using (1) and (2), and the $R$–$\gamma l$ behaviours of the corner pattern and face pattern phase conjugators should be something like that shown in Fig. 10.

At fixed power, when $\omega_0$ is small, both $\gamma' l'$ and $\gamma'' l''$ are small ($\gamma' l'$ is, however, always larger than $\gamma'' l''$). In this case, it can be seen from Fig. 10 that $R' > R''$. That is to say, the corner patterns correspond to a higher SPPC generation efficiency than the face patterns. As a result, corner patterns dominate in the phase conjugate. When $\omega_0$ is large, the contrary is true, the face patterns will dominate in the phase conjugator. At $\omega_0$ of medium size, the two beam patterns will generate phase-conjugate signal with comparable efficiency and they will appear in the phase conjugator alternately. The operation of the phase conjugator is not stable. Thus, the transition of the beam patterns is mainly due to the variation of $l$ with $\omega_0$. This variation changes the relative efficiencies generated by the two different beam patterns.

During the increase of $\omega_0$, other parameters in addition to $\gamma l$ should also change due to the decrease of light intensity: $\gamma_{2k}$ decreases. As a result, $M_{SPB}$ decreases with $\omega_0$. This may be the main reason as to why $R$ drops with increasing $\omega_0$ when $\omega_0$ is large. In the case of

+ $c$-face-incidence configuration (Fig. 6), however, the decrease of $\gamma_{2k}$ tends to increase the efficiency of the phase conjugator. Thus, the saturation and drop appear at much larger $\omega_0$.

The increase of the saturation power for $R$ with increasing $\omega_0$, as shown in Fig. 4, should also be due to the intensity dependence of $\gamma$ and $\gamma_{2k}$. The large $\omega_0$ is, $\gamma$ and $\gamma_{2k}$ saturate at higher $P$.

## 3 Conclusion

In summary, the power and beam-width dependences of the performances of a $BATiO_3$ : Ce crystal as self-pumped phase conjugators have been studied. In both $a$-face-incidence (corresponding to SPB-FWM mechanism) and + $c$-face-incidence (corresponding to TIR mechanism) configurations, $R$ is found to be sensitive to $\omega_0$ (at fixed $P$) or $P$ (at fixed $\omega_0$). Also with fixed $P(\omega_0)$, an optimum range of $\omega_0(P)$ exists for efficient operation of the phase conjugators.

In the $a$-face-incidence configuration, two different optical beam patterns have been observed: corner patterns and face patterns, and it was found that $\omega_0$ determines which beam patterns will appear in the phase conjugator. At small $\omega_0$ corner patterns appear in the phase conjugator. When $\omega_0$ becomes increased, face patterns will appear in it. This transition behaviour of beam patterns with $\omega_0$ is explained by considering the variation of the relative magnitudes of $R$ generated from the two beam patterns.

Of particular importance is the phenomenon that the SPB-FWM phase conjugator cannot arrive at steady state with $\omega_0$ of medium values. This phenomenon clearly demonstrates that one reason for unstable operation of some phase conjugators is the competition between different SPPC formation processes. Thus, the method to stabilize the phase conjugators' operations is to increase the efficiency difference of different processes.

With varying $\omega_0$ of $P$, different behaviours of $R$ have been obtained in a $a$-face-incidence and + $c$-face-incidence configurations. In addition, the time responses of the phase conjugation are also observed to be different. These differences are direct results of the different SPPC mechanisms. Comparative study of SPPC properties in the same crystal with different configurations, as exemplified in this paper, should be useful for us to understand the roles of different physical parameters in the operation of phase conjugators.

As self-pumped phase conjugators, $BaTiO_3$ : Ce crystals are efficient both in the visible and near infrared. Thus, they promise to have applications in many relating fields of nonlinear optics. The present as well as more comprehensive characterizations of SPPC properties of $BaTiO_3$ : Ce should be important and indispensable for its possible applications.

*Acknowledgements.* This research was supported by the National Natural Science Foundation of China, and by a grant for key research project (No. 2) in the Climbing Program from the State Science and Technology Commission of China.

## References

1. P. Günter, J.-P. Huignard (eds.): *Photorefractive Materials and their Applications I, II*, Topics Appl. Phys.,Vols. 61, 62 (Springer, Berlin, Heidelberg 1988, 1989)
2. P. Yeh: *Introduction to Photorefractive Nonlinear Optics* (Wiley, New York 1993)
   D.L. Hills: *Nonlinear Optics* (Springer, Berlin, Heidelberg 1991)
3. J.O. White, M. Cronin-Golomb, B. Fisher, A. Yariv: Appl. Phys. Lett. **40**, 450 (1982)
4. J. Feinberg: Opt. Lett. **7**, 486 (1982)
5. See, for example, N. Sonderer, P. Günter: J. Nonlinear Opt. Phys. **3**, 373 (1994)
6. T.Y. Chang, R.W. Hellwarth: Opt. Lett. **10**, 408 (1985)
7. M.H. Garrett, J.Y. Chang, H.P. Jensen, C. Warde: Opt. Lett. **18**, 405 (1993)
8. Y. Lian, H. Gao, P.X. Ye, Q. Guan, J. Wang: Appl. Phys. Lett. **73**, 495 (1993)
9. R.A. Mullen, D.J. Vickers, L. West, D.M. Pepper: J. Opt. Soc. Am. B **9**, 1726 (1992). From the beam patterns it seems that the meachanism is SPB-FWM
10. Y. Lian, S.X. Dou, H. Gao, Y. Zhu, X. Wu, C. Yang, P.X. Ye: Opt. Lett. **19**, 610 (1994)
11. Y. Zhu, C. Yang, M. Hui, X. Niu, J. Zhang, T. Zhou, X. Wu: Appl. Phys. Lett. **64**, 2341 (1994)
    C. Yang, Y. Zhu, M. Hui, X. Niu, H. Liu, X. Wu: Opt. Commun. **109**, 318 (1994). The SPPC mechanism in these references is actually SPB-FWM
12. R.A. Vazquez, R.R. Neurgaonkar, M.D. Ewbank: J. Opt. Soc. Am. B **9**, 1416 (1992)
13. C. Yang, Y. Zhang, P. Yeh, Y. Zhu, X. Wu: Opt. Commun. **113**, 416 (1995)
14. See, for example, M.C. Gower, P. Hribek: J. Opt. Soc. Am. B **5**, 1750 (1988)
15. See, for example, A.V. Nowak, T.R. Moore, R.A. Fisher: J. Opt. Soc. Am. B **5**, 1864 (1988)
16. M. Cronin-Golomb, B. Fisher, J.O. White, A. Yariv: IEEE J. QE-**20**, 12 (1984)
17. See, for example, K.R. MacDonald, J. Feinberg: J. Opt. Soc. Am. B **73**, 548 (1983)
18. M.H. Garrett, J.Y. Chang, H.P. Jensen, C. Warde: J. Opt. Soc. Am. B **9**, 1407 (1992)
19. See, for example, M. Snowbell, M. Horowitz, B. Fischer: J. Opt. Soc. Am. B **11**, 1972 (1994)
20. P. Yeh: Opt. Commun. **45**, 323 (1983)